Changes in Fly Ash With Thermal Treatment

John M. Fox

Degussa Admixtures, Inc., 23700 Chagrin Blvd., Cleveland, OH 44122-5554

KEYWORDS: fly ash, mineralogy, thermal treatment

ABSTRACT

Thermal beneficiation to remove carbon and ammonia makes coal fly ash marketable as a pozzolan for the concrete industry. The effect of these thermal treatments on the fly ash phase mineralogy (i.e. pozzolanic activity) may vary with ash composition. Fly ash samples with differing CaO contents were subjected to thermal treatment to evaluate changes in phase mineralogy. Samples were heated from 500 to1200 °C in 100 °C intervals. At each interval, loss on ignition (LOI), color, and X-ray diffraction mineralogy were determined.

Comparison of fly ash composition with the silica-alumina-lime ternary diagram reveals stable crystalline phases that should form on heating. The data shows that the temperature at which changes in phase composition occurs correlates with CaO content of the fly ashes. Class F fly ashes are the most refractory, with glass persisting to relatively high temperatures before additional mullite forms. As expected from the ternary diagram, fly ashes of intermediate lime content form feldspar and pyroxene at somewhat lower temperatures. High lime fly ashes (>20% CaO) crystallize melilite at even lower temperatures.

These data indicate that the low temperatures of ammonia burn out should result in minor changes in pozzolanic activity in most fly ashes. The potential effects of higher temperature carbon burn out on the pozzolanic activity of fly ashes should depend on the lime content and the maximum temperature. A loss of pozzolanic activity of high lime fly ash is possible.

INTRODUCTION

In recent years, changes at fossil fuel electric generating stations have been made to meet regulatory emissions standards. These changes can result in higher levels of carbon and ammonia in the fly ash. Higher levels of carbon are detrimental to air entrainment in concrete and ammonia may produce unacceptable levels of ammonia emission from the concrete. Ensuing changes in coal combustion products have prompted technological developments to maintain sufficiently low carbon and ammonia levels in fly ash for acceptability in its primary market—a pozzolan in concrete.

A variety of fly ash beneficiation strategies are being used; electrostatic and thermal systems are most common for carbon removal. Electrostatic carbon removal has been a viable commercial process since 1995 for converting high LOI fly ash to a useful concrete pozzolan.[1] Electrostatic carbon removal does not have the potential to reduce the glass phase in the ash (the phase primarily responsible for the pozolanic reaction) through devitrification, as it is not a thermal process.

Some commercial carbon burn-out (CBO) systems employ a fluidized bed combustor to thermally reduce carbon in all types of fly ash. Temperatures in the 700°C range with a residence time of 45 minutes are characteristic of the CBO process.[2,3] Thermal beneficiation of Class F fly ashes has being used commercially for over five years without agglomeration or compromising the strength-producing characteristics in concrete.[4] This implies little change in the amount and nature of the glass phase in Class F fly ashes processed by CBO.

Studies on the effects of thermal treatment of fly ash show that a significant portion of active carbon was removed with little change in the inorganic portion of a Class F fly ash up to 500°C. By 769°C all carbon was removed, however, the glassy background on the X-ray pattern was lower and it was concluded that changes in the inorganic phases must be ocurring.[5]

Where ammonium salts exceed 100 ppm in fly ash, chemical treatment is necessary and has been successfully used for commercial beneficiation.[1] Thermal beneficiation systems used primarily for removal of ammonium salts operate at relatively low temperatures compared with CBO units.[6] One thermal ammonia process involves exposing fly ash to preheated air (as high as 927°C (1701°F)) until the fly ash reaches at least 482°C (900°F), at which temperature ammonium compounds become volatile and are removed.[7]

The increasing use of dry flue gas desulfurization (FGD) systems that employ sorbent injection ($Ca(OH)_2$ or CaO) upstream of ash precipitators has led to interest in the possibility of using the resulting "clean-coal ash" in concrete. These lime and sulfur-enhanced fly ashes, known as spray dryer ashes, generally do not meet all ASTM C 618 specifications,[8] however, have shown promise for certain concrete applications.[9]

In this work, four commercially available fly ashes covering a wide range of compositions were thermally treated to determine the kinds of phase changes that may

occur at temperatures at and above those expected in CBO or ammonia removal processes. Changes in thermally treated fly ash that may impact its usefulness as a pozzolan in concrete are discussed.

MATERIALS

Four commercially available fly ashes were selected for thermal treatment. Ash 1 is from a Pennsylvania plant burning Carboniferous bituminous coal from West Virginia. Ash 2 is from a Washington plant burning Eocene subbituminous Skookumchuck coal. Ash 3 is a spray dryer ash from a Nevada plant burning Cretaceous bituminous coal from the Wasatch Plateau and using dry FGD technology. Ash 4 is from a Colorado plant burning subbituminous coal from the Powder River Basin in Wyoming. The chemical composition of the fly ashes is shown in Table 1.

Table 1. Chemical Analysis of Fly Ashes

Oxide Wt. %	Ash 1	Ash 2	Ash 3	Ash 4
SiO_2	47.97	49.63	44.38	31.60
Al_2O_3	23.79	24.14	12.52	18.58
Fe_2O_3	15.79	7.99	3.44	5.58
CaO	3.72	7.55	18.50	28.29
MgO	0.92	1.64	4.44	6.82
SO_3	0.51	0.36	8.55	2.57
Na_2O	0.77	2.44	2.35	2.01
K_2O	1.77	0.61	0.98	0.31
TiO_2	1.16	3.98	0.77	1.44
P_2O_5	0.34	0.75	0.24	1.09
Mn_2O_3	0.04	0.06	0.03	0.04
SrO	0.14	0.29	0.10	0.50
Cr_2O_3	0.03	0.02	0.02	0.02
ZnO	0.02	0.02	<0.01	0.01
Alkalis as Na_2O eq.	1.93	2.84	2.99	2.22
Free H_2O	0.31	0.14	0.49	0.11
SiO_2+Al_2O_3+Fe_2O_3	87.5	81.8	60.3	55.8

ASTM C 618 classifies fly ash chemically and by coal rank. Class F fly ashes contain at least 70% by weight $SiO_2 + Al_2O_3 + Fe_2O_3$ and are typically the product of burning high-rank coals (bituminous and anthracite). Class C fly ashes contain a minimum of 50% by weight of $SiO_2 + Al_2O_3 + Fe_2O_3$ and a cementitious component, and are normally a product of burning low-rank coals (lignite and subbituminous).[8]

Ash 1 is a typical low-lime Class F fly ash. Ash 2 meets the Class F specification; however, it is from a subbituminous coal and nearly contains enough CaO to be classified as an intermediate (CI) fly ash in the Canadian Standards Association's CSA A23.[10] Ash 3 is a spray dryer ash that would be considered a Class C fly ash on bulk composition, but does not meet C 618 on total sulfur (> 5% SO_3) and has no significant cementitious properties. Ash 4 is a typical high-lime Class C fly ash.

FLY ASH THERMAL TREATMENT AND ANALYSIS

Splits of the four fly ash samples were heated in a thermocouple-controlled muffle furnace at a rate of 15 °C per minute to maximum temperatures of 500°C, 600 °C, 700 °C, 800°C, 900 °C, 1000 °C, 1100 °C, and 1200 °C. Splits were kept at the maximum temperature for one hour, removed, and quickly cooled to room temperature and immediately processed without storage in a dessicator. The loss on ignition (LOI) was determined for each temperature level for all samples according to ASTM C 311.

The unheated fly ashes and each of the thermally treated splits were ground in a McCrone Micronizer with isopropyl alcohol, dried, and subjected to X-ray diffraction (XRD) analysis using copper radiation with a step size of 0.02 degrees and 1-second count time. Pattern processing was done using JADE software and the ICDD pattern database. The glass index (GI), an index of the relative amount of amorphous material in each sample, was calculated according to the equation GI = (P-C)/P, where P is the total pattern integrated counts less background and C is the total pattern counts after subtracting background and amorphous material. Reported values are averages of fitting each pattern four times. The GI is not a quantitative glass determination, rather it is a simple ratio of glass counts to total glass plus crystalline materials counts which can be used to compare samples. Smaller values indicate less amorphous material and values in the hundredths indicate essentially no glass. The glass "peak" centroid was also determined as an average from four peak fits.

Colors were determined after micronizing by comparison with the Munsell color chart. The degree of sintering was given a rating of 0 to 5, with 0 being unsintered loose powder and 5 being very, very hard to partially fused.

RESULTS

The XRD patterns of thermally treated splits of each fly ash are shown overlain in Figures 1 to 4. The key line of each important phase has been colored. Tables 2 to 5 show a summary of the glass index (GI), LOI, sinter, color, and important phase changes with temperature for each fly ash. These tables summarize the main XRD-phase mineralogy as the temperature increases and the glass is consumed.

Ash 1 has a phase mineralogy typical for Class F fly ashes where magnetite is present with hematite in addition to abundant mullite and quartz. The CaO is present as a small amount of crystalline anhydrite and in the glass. Thermal treatment causes mullite and a small amount of plagioclase to crystallize at the highest temperatures. Magnetite is oxidized to hematite. The glass centroid is at 24.3 °2Θ and shifted to lower angles with temperature, particularly at 1000°C and above.

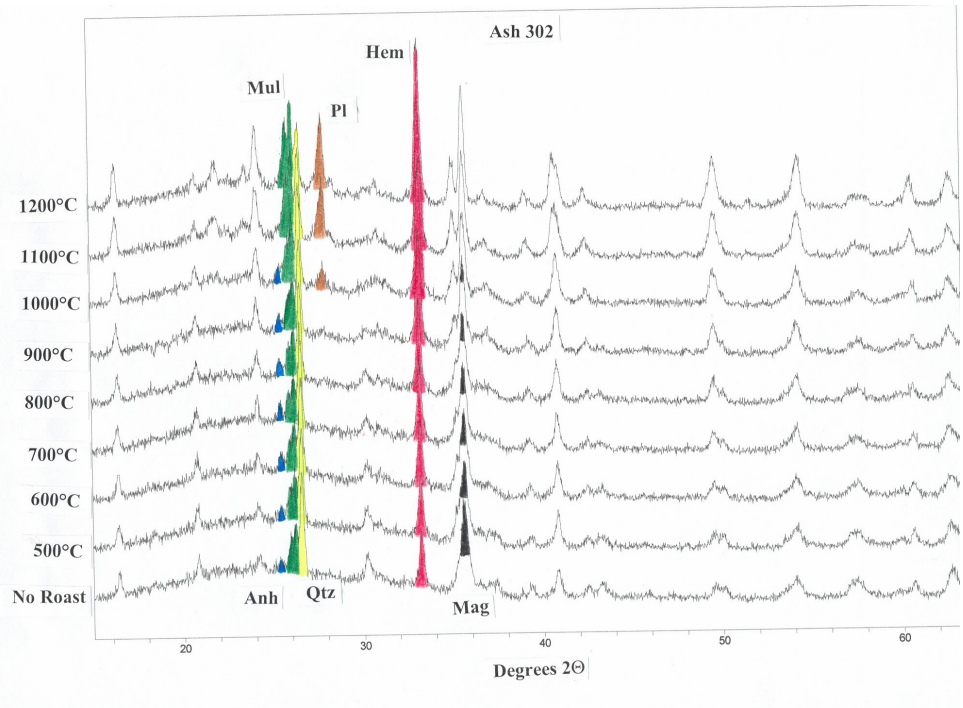

Figure 1. Important phase changes seen in XRD patterns of Ash 1 (Anh = anhydrite, Mul = mullite, Qtz = quartz, Pl = plagioclase, Hem = hematite, Mag = magnetite).

Table 2. GI, LOI, Sinter, Color, and crystalline phase changes with temperature for Ash 1 (white box indicates not present, gray box indicates appearance or disappearance, black box indicates continued presence).

Temp °C	GI	LOI/Sinter	Color	magnetite	hematite	Anhydrite	Plagioclase	mullite	quartz
1200	.27	3.2 / 5	5YR 4/4 reddish brown						
1100	.27	3.0 / 4	7.5YR 4/4 dark brown						
1000	.32	2.7 / 3	7.5YR 4.5/4 brown						
900	.33	2.6 / 2	7.5YR 5/4 brown						
800	.35	2.7 / 1	10YR 4.5/3 brown						
700	.37	2.6 / 0	10YR 5/5 yellowish brown						
600	.38	2.1 / 0	10YR 5/4 yellowish brown						
500	.38	1.1 / 0	10YR 5/4 yellowish brown						
Not heated	.37	- / -	10YR 4.5/3 brown						

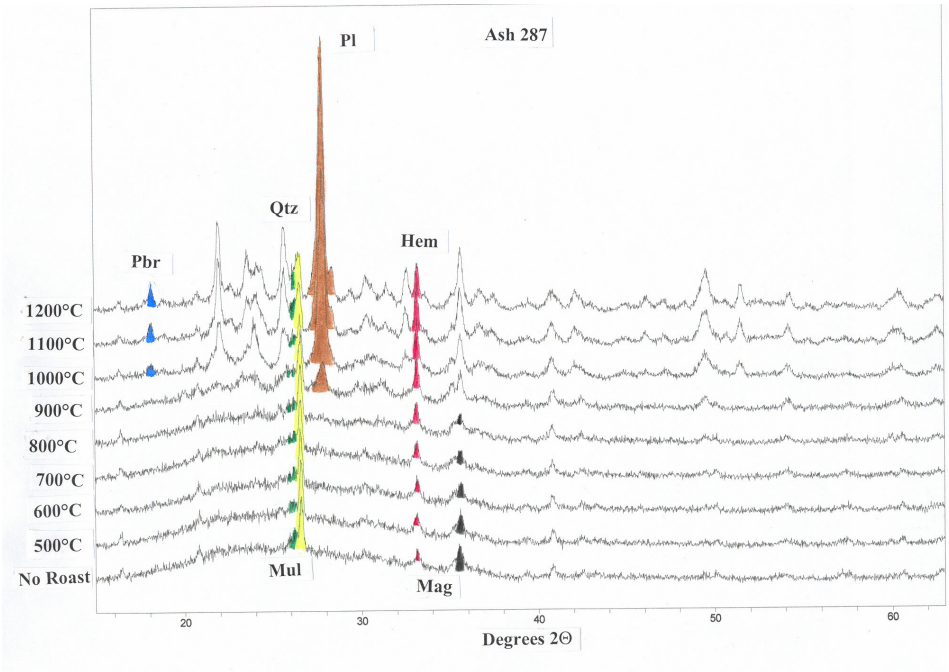

Figure 2. Important phase changes seen in XRD patterns of Ash 2 are colored. (Pbr = pseudobrookite, Mul = mullite, Qtz = quartz, Pl = plagioclase, Hem = hematite, Mag = magnetite.)

Table 3. GI, LOI, Sinter, Color, and crystalline phase changes with temperature for Ash 2 (white box indicates not present, gray box indicates appearance or disappearance, black box indicates continued presence).

Temp °C	GI	LOI/Sinter	Color	magnetite	hematite	plagioclase	mullite	quartz	pseudobrookite
1200	0.20	0.9 / 5	10YR 6/6 brownish yellow						
1100	0.22	0.9 / 4	10YR 5/6 yellowish brown						
1000	0.26	0.8 / 4	10YR 5.5/5 light yellowish brown						
900	0.41	0.5 / 3	7.5YR 5/4 brown						
800	0.51	0.6 / 1	10YR 6/4 light yellowish brown						
700	0.55	0.5 / 0	10YR 6/3.5 light yellowish brown						
600	0.52	0.6 / 0	10YR 6/3 pale brown						
500	0.55	0.6 / 0	10YR 6/3 pale brown						
Not heated	0.55	- / -	10YR 5/2 grayish brown						

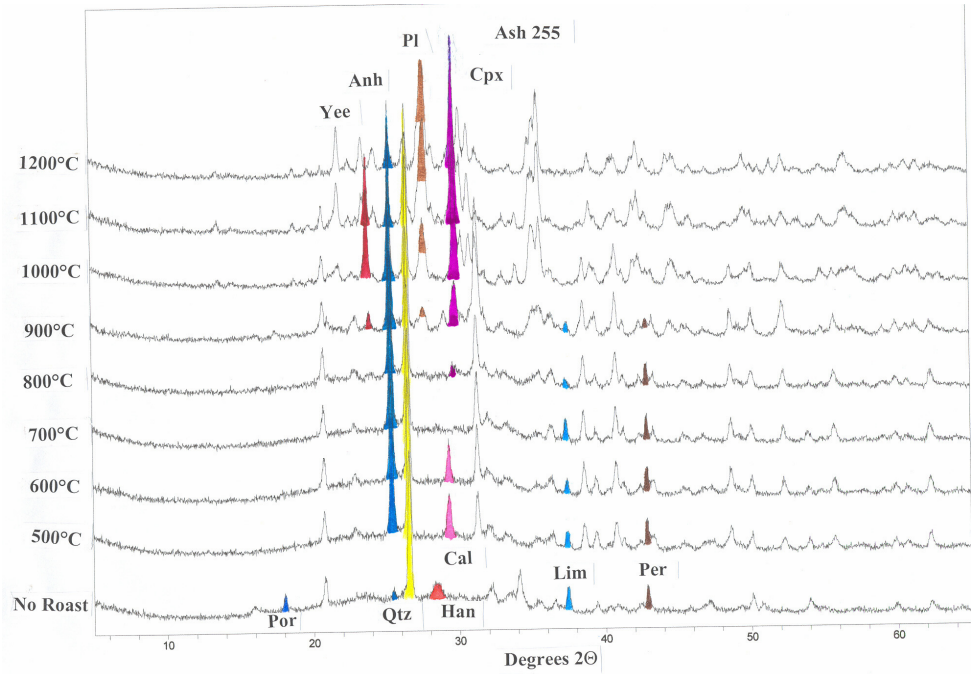

Figure 3. Important phase changes seen in XRD patterns of Ash 3 are colored (Por = portlandite, Yee = yeelimite, Anh = anhydrite, Qtz = quartz, Pl = plagioclase, Han = hannebachite, Cal = calcite, Cpx = clinopyroxene, Lim = lime, Per = periclase.)

Table 4. GI, LOI, Sinter, Color, and crystalline phase changes with temperature for Ash 3 (white box indicates not present, gray box indicates appearance or disappearance, black box indicates continued presence).

Temp °C	**GI**	**LOI/Sinter**	**Color**	portlandite	hannebachite	calcite	lime	periclase	anhydrite	plagioclase	yeelimite	clinopyroxene	quartz
1200	.14	8.9 / Fused	10YR 8/3.5 very pale brown										
1100	.09	8.9 / 2	10YR 8/4 very pale brown										
1000	.09	4.4 / 2	10YR 8/2.5 very pale brown										
900	.15	4.1 / 2	10YR 8/2 white										
800	.30	4.1 / 1	10YR 7/2 light gray										
700	.30	3.9 / 0	10YR 7/2 light gray										
600	.33	2.7 / 0	10YR 7/1.5 light gray										
500	.32	2.0 / 0	10YR 7/1.5 light gray										
Not heated	.40	- / -	10YR 5/1 gray										

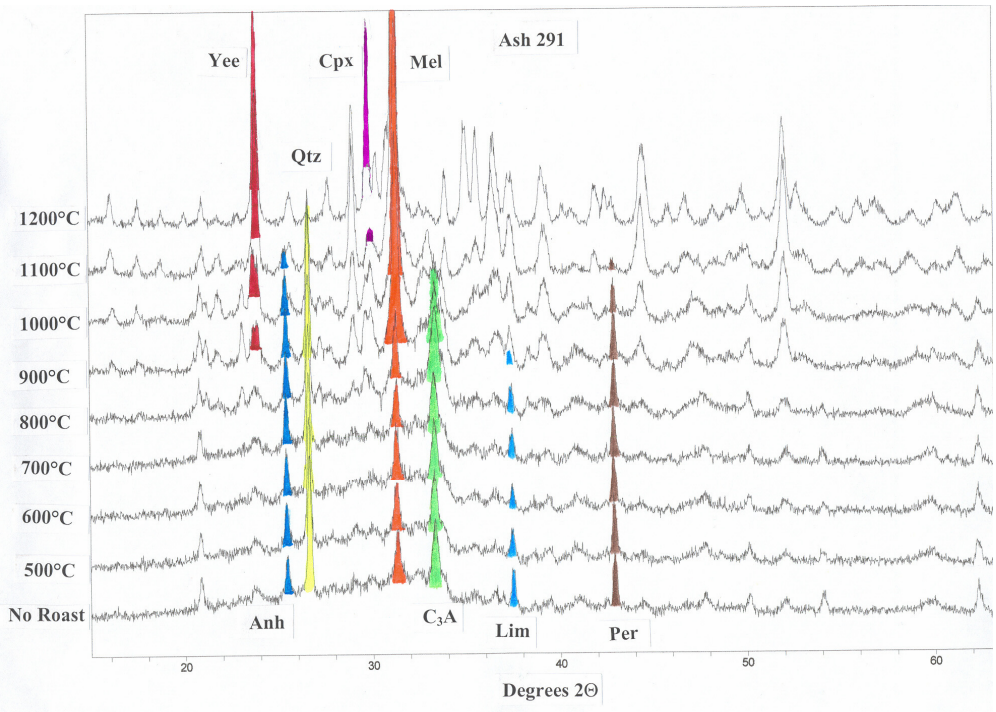

Figure 4. Important phase changes seen in XRD patterns of Ash 4 are colored (Yee = yeelimite, Anh = anhydrite, Qtz = quartz, Cpx = clinopyroxene, Mel = melilite, Lim = lime, Per = periclase.)

Table 5. GI, LOI, Sinter, Color, and crystalline phase changes with temperature for Ash 4 (white box indicates not present, gray box indicates appearance or disappearance, black box indicates continued presence).

Temp °C	**GI**	**LOI/Sinter**	**Color**	anhydrite	lime	periclase	C_3A	yeelimite	clinopyroxene	melilite	quartz	nepheline	hercynite
1200	.01	1.4 / 5	10YR 7/4 very pale brown					■	■	■	▒		
1100	.01	1.1 / 3	10YR 7/6 yellow	▒		▒		■	▒	■	■		■
1000	.03	0.6 / 2	10YR 6.5/5 light yellowish brown	▒		■	▒	■		■	■	■	
900	.07	0.6 / 2	10YR 6/3 pale brown	■	▒	■	▒	▒		■	■	■	
800	.23	0.6 / 1	10YR 7/3 very pale brown	■	■	■	■	▒		■	■	■	
700	.32	0.6 / 0	10YR 6.5/3 very pale brown	■	■	■	■			■	■		
600	.32	0.4 / 0	10YR 7/3 very pale brown	■	■	■	■			■	■		
500	.32	0.3 / 0	10YR 7/4 very pale brown	■	■	■	■			■	■		
Not heated	.31	- / -	10YR 7.5/3 very pale brown	■	■	■	■			■	■		

Ash 2 has a typical phase mineralogy of a Class F fly ash. Magnetite (Fe_3O_4) is the dominant iron oxide with some hematite (Fe_2O_3) present. Mullite ($Al_6Si_2O_{13}$) and quartz (SiO_2) are also characteristic. This ash contains more CaO than Ash 1, but the CaO is primarily in the glass phase. Thermal treatment converts magnetite to hematite, while plagioclase and pseudobrookite (Fe_2TiO_5) crystallize. The formation of abundant plagioclase sets this ash apart from a true Class F low-lime pulverized fuel ash like Ash 1. The glass centroid is at 25.4 °2Θ, and does not become notably smaller with increasing temperature.

Abundant calcium and sulfur containing phases present in Ash 3 are a result of the dry FGD process. Portlandite ($Ca(OH)_2$), hannebachite ($CaSO_3$ 0.5 H_2O), lime (CaO), anhydrite ($CaSO_4$), and periclase (MgO) are present in the fly ash as received. Thermal treatment results in the formation of abundant anhydrite, plagioclase feldspar ($(Na,Ca)Al(Si,Al)_2O_6$), yeelimite ($Ca_4Al_6O_{12}SO_4$), and clinopyroxene. Calcite ($CaCO_3$), appears after heating to 500°C and 600°C, but this is somewhat unexpected. Yeelimite shows line shift indicative of sodium substitution and matches the related sodalite group zeolite structure type hauyne (ICDD file 37-0473). The clinopyroxene is a close match with diopside ($Ca(Mg,Al)(Si,Al)_2O_6$) and may be a solid solution with esseneite ($CaFe_{0.6}Al_{1.3}SiO_6$). The glass has a centroid of 26.8°2Θ, with somewhat lower values with higher treatment temperature.

Ash 4 is a typical Class C fly ash containing the cementitious component C_3A ($Ca_3Al_2O_6$). As Powder River Basin coals contain abundant organic calcium and magnesium, lime and periclase are ash phases. Anhydrite, quartz, and a small amount of melilite are present. The melilite phase most closely matching the XRD lines is gehelenite ($Ca_2Al_2SiO_7$). Merwinite ($Ca_3Mg(SiO_4)_2$) may be present but in an amount significantly lower than C_3A; this is difficult to resolve due to overlap on the high angle side of the C_3A peak. Thermal treatment stabilizes a large amount of crystalline gehelenite, some yeelimite, and clinopyroxene at the highest temperature. Yeelimite and clinopyroxene are structurally similar in line positions to that in Ash 3. Hercynite (Al_2FeO_4) is also present at 1100 °C, but is known to be a stable spinel observed only between 1000°C and 1200°C.[11,12] Lines matching nepheline ($K(Na,K)_3Al_4Si_4O_{16}$) (ICDD file 09-0338) are present from 800°C to 1000°C, with the maximum at 900°C. Nepheline has been previously identified in 1000°C ash from the Absaloka subbituminous coal from Montana.[13] The C_3A is relatively stable, persisting until 800°C after which it begins to decrease and disappears by 1100°C. The glass centroid is at 29.3°2Θ and can not be effectively measured by 1000°C due to the small percent of glass remaining.

Color changes in the fly ash samples are most pronounced at 500°C and 900°C. A lighter color results from heating to 500°C in all samples except Ash 4. In most fly ashes the oxidation of carbon results in a lighter color. The initial stabilization of a relatively small amount of crystalline melilite may be the cause of the minor darkening of Ash 4 on heating to 500°C. A color change between 800°C and 900°C corresponds to the crystallization of phases stabilized as the glass content is reduced. The color change and loss of glass is much more gradual for Ash 1 and much of the color change involves oxidation of magnetite.

The standard procedure for LOI given in ASTM C 114-05 specifies a heating temperature of 950°C±50°C, which is reduced for fly ash in ASTM C 311-04 to 750°C±50°C. The LOI data shows a region of relative stability from 700°C to 900°C. Between 900°C and 1000°C the LOI increases somewhat for all samples except Ash 3 which increases abruptly with the decomposition of anhydrite.

Sintering, the degree of bonding between particles, increases progressively after 800°C for all samples except Ash 3, which changes from a weak sinter at 1100°C to total fusion at 1200°C.

DISCUSSION

As an index of glass abundance, changes in GI values show the temperature at which glass becomes of sufficiently low viscosity for the transformation to crystalline phases to occur. This involves very short induction times of nucleation and crystallization and can occur rapidly (in as little as 10 minutes at 1000°C).[14] The glassy stability ratio (GSR) is the ratio of the weight percent ratio of glass-network-former oxides to glass-network-modifier oxides ($SiO_2/\Sigma(Na_2O + K_2O + CaO + MgO + Al_2O_3)$. Lower GSR values are characteristic of glasses with a greater tendency to crystallize or devitrify on heating.[14] Figure 5 shows that Ash 1 has a gradual decrease in glass content starting at 700°C to 800°C while Ash 2 has a sharp drop. Ash 3 shows a sharp decrease in glass after 800°C and becomes almost completely crystalline by 1000°C. The fused glass of Ash 3 at 1200°C is unstable and becomes more crystalline on cooling. Ash 4 shows a strong decrease in glass between 700°C and 800°C and is almost fully crystalline at 1000°C. Comparison of the GSR and the GI at 1000°C in Figure 5 reveals a strong correlation between the two. In these ashes, CaO is the primary contributor to GSR which underscores the importance of CaO on the degree of devitrification with temperature. Regardless of the relative amount of glass compared to crystalline phases in the original fly ash, the greater the CaO, the more crystallized and the less glassy is the sample after heating to 1000°C and above. At higher values of GSR in Ash 1, the glass remains very stable and shows relatively little devitrification in the range of temperatures studied; at lower GSR values the glass in the other ashes is less stable and more readily devitrifies.

The fly ashes used in this study are plotted on the silica-alumina-lime ternary phase diagram in Figure 6. The bulk chemical composition of the ashes falls within the mullite, plagioclase-clinopyroxene, and melilite fields of stability. Although the boundaries and fields are modified with the addition of other elements, this diagram is a reasonable approximation of phases observed in devitrified fly ash glasses, as mullite, plagioclase, and melilite remain stable phase regions as CaO increases. For example, the addition of magnesium to the system causes a strong reduction in the wollastonite field in favor of pyroxene, yet the mullite, plagioclase, and melilite fields remain.[15] The most important stable phases at the higher temperature thermal treatments are as expected from the bulk chemistry of the fly ashes. Low lime fly ashes are thermally stable and crystallize mullite; Intermediate lime fly ashes (8% to 20% CaO) are of intermediate stability and

crystallize plagioclase and clinopyroxene; high lime fly ashes are the least stable thermally and crystallize melilite.

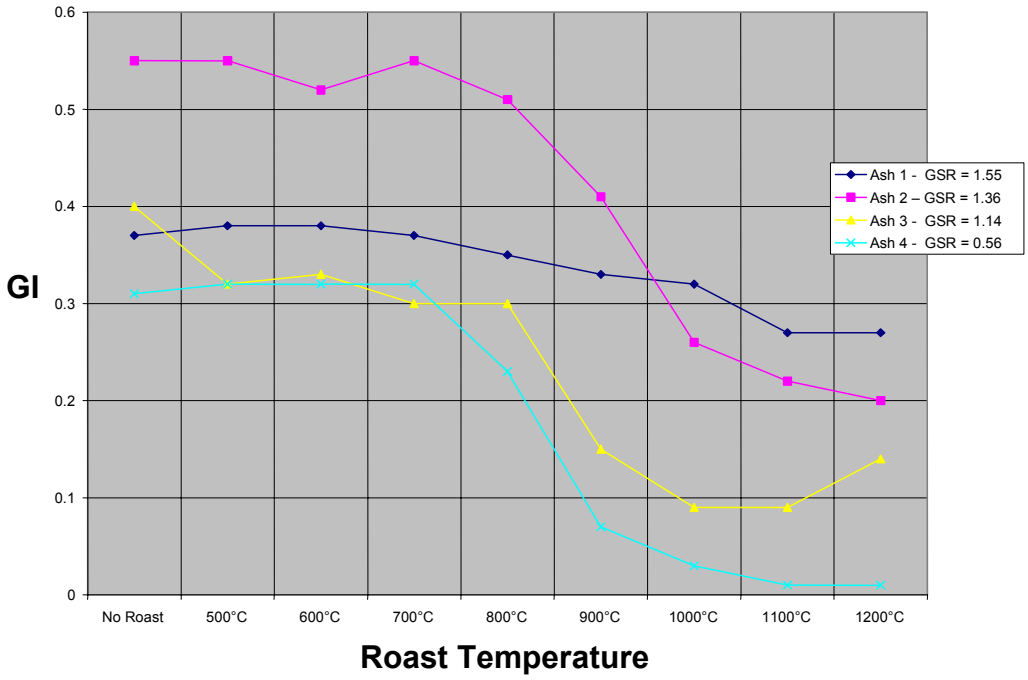

Figure 5. The glass index plotted against roast temperature for the four different fly ashes.

Glass content is one of the most important characteristics of fly ash that influence its value as a pozzolan in concrete. Crystalline phases in fly ash are thought to contribute little to pozzolanic reactivity.[17, 18] While the thermal history of fly ash may impact the pozzolanic activity through changes in residual strain of larger particles,[18] clearly, any process that leads to a reduction in the glass content of fly ash could lower its effectivity as a pozzolan in concrete. In this work, changes in fly ashes from bituminous and subbituminous coals having a range of CaO contents have been documented for thermal treatment through the region of critical glass devitrification. The process of devitrification in fly ash glass is similar to the glass ceramic process in which thermal treatment of rapidly quenched glass causes nucleation and growth of crystalline phases.[14] A number of investigators have considered changes in ash fusion temperatures as a function of fly ash chemistry and fairly low sintering and fusion temperatures (550-600 °C) are reported to be possible in relatively short times (as low as 10 minutes).[19-23]

The present work shows the importance of composition in the devitrification of thermally treated fly ash. Ash 1 is a typical Class F ash with very low CaO and a refractory nature with little potential for reduced pozzolanic activity in concrete when processed at typical CBO temperatures. Although from a subbituminous coal, Ash 2 is also marketed as a Class F fly ash, however, it is intermediate in composition with enough CaO to cause it to

be more readily devitrified to plagioclase. Although the product of bituminous coal combustion, Ash 3 contains abundant absorbed calcium compounds from the spray dryer process, making it a hybrid fly ash with a low fusion point. Ash 4 is a typical high CaO Class C fly ash resulting from burning subbituminous coal of the Powder River Basin and contains cementitious C_3A. Ash 4 is prone to rapid and nearly complete devitrification to melilite, among other non-pozzolanic crystalline alkali metal-containing aluminosilicates, at temperatures between 700°C and 800°C; between 900°C and 1000 the cementitious component (C_3A) is lost.

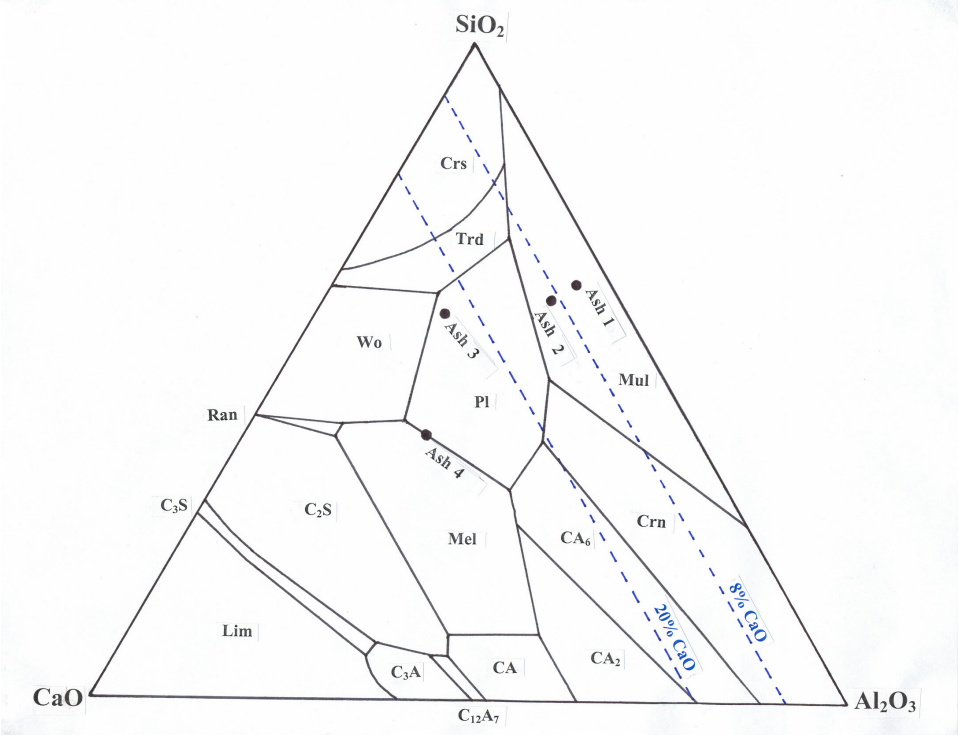

Figure 6. The generalized silica-alumina-lime ternary diagram shows the location of the fly ashes with respect to phase boundaries and the position of the 8% CaO and 20% CaO lines. Crs = cristobalite, Trd = tridymite, Mul = mullite, Pl = plagioclase, Wo = wollastonite, Crn = corundum, CA_6 = hibonite, CA_2 = grossite, CA = calcium aluminate, $C_{12}A_7$ = mayenite, C_3A = tricalcium aluminate, Lim = lime, C_3S = tricalcium silicate (alite), C_2S = larnite (belite), Ran = rankinite, and Mel = melilite. Phase boundaries are drawn from Dunstan, 1980 [16].

CONCLUSIONS

Based on the four fly ashes studied the following conclusions are drawn:

1. Thermal treatment of fly ashes indicates changes in color, LOI, degree of sintering, and phase mineralogy become significant above 700°C.
2. Fly ashes with higher CaO contents are more likely to devitrify at lower temperatures and more completely than those with lower CaO.
3. Up to 700°C, little glass devitrification occurred indicating that CBO process temperatures should not significantly reduce the pozzolanic activity of fly ash in concrete.
4. At temperatures between 700°C and 800°C high lime fly ashes (>20% CaO) experience significant glass devitrification, that could result in reductions in pozzolanic activity. The cementitious phase in Class C fly ash (C3A) is only affected at temperatures higher than 900°C.
5. Ammonia burn out temperatures are too low to affect the pozzolanic activity of fly ash.

REFERENCES

[1] Bittner, J.D., Gasiorowski, S.A., and Hrach, F.J., Carbon Separation and ammonia removal at Jacksonville Electric St. Johns River Power Park, Proceedings, 2003 International Ash Utilization Symposium, 2003.

[2] Giampa, V.M., The fate of ammonia and mercury in the carbon burn-out (CBO^{TM}) process, International Fly Ash Utilization Symposia, 18-21 October 2003, Lexington, Kentucky, USA.

[3] Frady, W.T., Keppeler, J.G., and Knowles, J.C., South Carolina Electric & Gas successful application of carbon burn-out at the Wateree Station, International Fly Ash Utilization Symposia, 18-20 October 1999, Lexington, Kentucky, USA.

[4] Keppeler, J.G., Carbon burn-out, commercialization and experience update, Proceedings: 15th International American Coal Ash Association Symposium on Management & Use of Coal Combustion Products (CCPs), 2003, pp.45-1 to 45-6.

[5] LaCount, R.B., Baltrus, J., Banfield, T.L., Diehl, J.R., Frommell, E.A., Giles, K.A., Irdi, G.A., Kern, D.G., Leyda, T.A., Martello, D.V., and Tamilia, J.P., Treatment of high carbon fly ash to produce a low foam index product with carbon content retained, Proceedings: 14th International Symposium on Management and Use of Coal Combustion Products (CCPs), 2001, Vol. 1, pp. 15-1 to 15-13.

[6] Ramme, B.W. and Fisher, B.C., Ash beneficiation through Wisconsin Electric Power Company's ammonia liberation process, Proceedings: 14th International Symposium on

Management and Use of Coal Combustion Products (CCPs): Volume 1, EPRI, Palo Alto, CA: 2001.

[7] Ramme, B.W. and Fisher, B.C., Ammonia removal from fly ash, U.S. Patent No. 6,755,901, June 29, 2004.

[8] ASTM C 618 –03, Standard Specification for Coal Fly Ash and Raw or Calcined Natural Pozzolan for Use in Concrete, 2003.

[9] Wu, Z. and Naik, T.R., Use of clean-coal ash for managing ASR constructed since 1984, Presentation at ACI meeting, Spring, 2004, Washington, D.C., University of Wisconsin Report No. CBU-2004-06.

[10] Thomas, M.D.A., The use of fly ash in concrete: a question of classification, Proceedings, 1997 International Ash Utilization Symposium, 1997, Lexington, KY, U.S.A.

[11] Querol, X., Fernandez T.J.L., and Soler, A.L., The behaviour of mineral matter during combustion of Spanish subbituminous and brown coals, Mineralogical Magazine, March 1994, Vol. 58, pp. 119-133.

[12] Huffman, G.P. and Huggins, F.E., Reactions and transformations of coal mineral matter at elevated temperatures, In: Mineral Matter and Ash in Coal, ACS Symposium Series 301, (Ed K.S. Vorres, editor), 1986, pp. 100-113.

[13] Falcone, S.K. and Schobert, H.H., Mineral transformations during ashing of selected low-rank coals, In: Mineral Matter and Ash in Coal, ACS Symposium Series 301, (Ed K.S. Vorres), 1986, pp. 114-127.

[14] Barbieri, L., Lancellotti, I., Manfredini, T., Pellacani, G.C., Rincon, J.M., and Romero, M., Nucleation and crystallization of new glasses from fly ash originating from thermal power plants, Journal of the American Ceramic Society, 2001, Volume 84, No. 8, pp. 1851-1858.

[15] Kalmanovitch, D.P. and Williamson, J., Crystallization of coal ash melts, In: Mineral Matter and Ash in Coal, American Chemical Society, 1986.

[16] Dunstan, E.R., Jr., A possible method for identifying fly ashes that will improve the sulfate resistance of concretes, Cement, Concrete, and Aggregates, 1980, Vol. 2, No. 1, pp. 20-30.

[17] Malhotra, V.M. and Ramezanianpour, A.A., Fly Ash in Concrete, 2nd edition, 1994, CANMET MSL 94-45(1R), 307 pp.

[18] Helmuth, R., Fly Ash in Cement and Concrete, 1987, Portland Cement Association, 203 pp.

[19] Al-Otoom, A.Y., Elliott, L.K., Moghtaderi, B., and Wall, T.F., The sintering temperture of ash agglomeration, and defluidisation in a bench scale PFBC, Fuel, 2005, Vol. 84, pp. 109-114.

[20] Winegartner, E.C. and Ubbens, A.A., Understanding coal ash quality parameters, Transactions, Society of Mining Engineers, AIME, 1976, Vol. 260, pp. 67-70.

[21] Raask, E., Flame Vitrification and sintering characteristics of silicate ash, In: Mineral Matter and Ash in Coal, ACS Symposium Series 301, (Ed K.S. Vorres), 1986, pp. 138-115.

[22] Huggins, F.E., Kosmack, D.A, and Huffman, G.P., Correlation between ash-fusion temperatures and ternary equilibrium diagrams, Fuel, 1981, Vol. 60, pp. 577-584.

[23] Ely, F.G. and Barnhart, D.H., Coal ash – its effect on boiler availability, In: Chemistry of Coal Utilization (Supplementary Volume) (Ed H.H. Lowry) J. Wiley and Sons, New York, 1963, Chapter 19, pp. 820-891.